Oscillatory magnetoresistance in nanopatterned superconducting $La_{1.84}Sr_{0.16}CuO_4$ films

I. Sochnikov,[1] A. Shaulov,[1] Y. Yeshurun,[1] G. Logvenov,[2] and I. Božović[2]

[1]*Department of Physics, Institute of Superconductivity and Institute of Nanotechnology and Advanced Materials, Bar-Ilan University, Ramat-Gan 52900, Israel*

[2]*Brookhaven National Laboratory, Upton, New York 11973-5000, USA*

(Received 17 June 2010; revised manuscript received 27 August 2010; published 21 September 2010)

A superconducting $La_{1.84}Sr_{0.16}CuO_4$ film patterned into a network of 100×100 nm^2 noninteracting square loops exhibits large magnetoresistance oscillations superimposed on a background which increases monotonically with the applied magnetic field. Neither the oscillations amplitude nor its temperature dependence can be explained by the Little-Parks effect. Conversely, a good quantitative agreement is obtained with a recently proposed model ascribing the oscillations to the interaction between thermally excited moving vortices and the oscillating persistent currents induced in the loops. Extension of this model, allowing for direct interaction of the vortices and antivortices magnetic moment with the applied field, accounts quantitatively for the monotonic background as well. Analysis of the background indicates that in the patterned film both vortices and antivortices are present at comparable densities. This finding is consistent with the occurrence of Berezinskii-Kosterlitz-Thouless transition in $La_{1.84}Sr_{0.16}CuO_4$ films.

DOI: 10.1103/PhysRevB.82.094513 PACS number(s): 74.78.Na, 74.25.Uv, 74.25.Wx

I. INTRODUCTION

Quantization of the fluxoid in multiply connected superconductors was first predicted by Fritz London in the early days of superconductivity.[1] This prediction was later confirmed experimentally by Little and Parks[2–4] who demonstrated that a thin-walled superconducting cylinder pierced by a magnetic flux shows magnetoresistance oscillations with the period equal to the superconducting flux quantum $\Phi_0=h/2e$. The explanation provided by Little and Parks was that the resistance oscillations $\Delta R(H)$ reflect periodic changes in the superconducting transition temperature T_c given by $\Delta T_c=\Delta R(H)(dT/dR)$. Subsequent studies have demonstrated periodic changes in the magnetoresistance also in two-dimensional (2D) networks of superconducting wires (see Refs. 5 and 6, and references therein). These studies were focused on determining the arrangements of vortices in the network and the effects of size and symmetry of the network on the periodic oscillations.

Magnetoresistance oscillations in a high-T_c superconducting network were first reported by Gammel *et al.*,[7] who ascribed them to the Little-Parks effect. However, the amplitude of the oscillations and its temperature dependence could not be accounted for while no attempt was made to analyze the monotonic background on which the magnetoresistance oscillations were superimposed.

We have recently demonstrated[8] large magnetoresistance oscillations in a network of decoupled 150×150 nm^2 $La_{1.84}Sr_{0.16}CuO_4$ loops and showed that the oscillations amplitude is much larger than what one would expect from the periodic changes in the critical temperature associated with the Little-Parks effect. We ascribed these oscillations to a dynamic effect: thermally excited vortices move and interact with the persistent current induced in the loops by the magnetic field. As the induced current oscillates periodically with the magnetic flux piercing the loops, due to fluxoid quantization, this interaction is periodic with the applied magnetic field; this gives rise to the magnetoresistance oscillations. This effect is especially important in high-T_c superconductors, where the Little-Parks effect is suppressed because of the relatively small coherence length, while the vortex dynamics is enhanced due to relatively large thermal fluctuations. As the size of the loops decreases down to the nanoscale, the dynamic effect becomes even more significant, because of an increase in the persistent current induced in the loops. We have also outlined a theoretical analysis[8] based on the fluxoid dynamics model,[9,10] that successfully accounts for the amplitude of the observed magnetoresistance oscillations and its temperature dependence.

In this paper we present data on smaller $La_{1.84}Sr_{0.16}CuO_4$ loops of size 100×100 nm^2, almost an order of magnitude smaller than what has been reported previously for other high-T_c materials. In addition, we extend our theoretical analysis to include description of the monotonic background on which the magnetoresistance oscillations are superimposed. The analysis of the magnetoresistance background provides evidence for the presence of both vortices and antivortices in $La_{1.84}Sr_{0.16}CuO_4$ films at elevated temperatures. This is consistent with thermal generation of vortex-antivortex pairs that dissociate above a certain temperature, the so-called Berezinskii-Kosterlitz-Thouless (BKT) transition point.[11] The occurrence of a BKT transition has been predicted in thin high-T_c superconducting films with the lateral dimensions smaller than the perpendicular penetration depth.[12] However, the experimental efforts to observe such a phase transition in superconductors have so far yielded inconclusive results.

II. EXPERIMENTAL

An advanced molecular-beam epitaxy system was employed to synthesize optimally doped $La_{1.84}Sr_{0.16}CuO_4$ films, 26 nm thick, epitaxially on $LaSrAlO_4$ substrates polished perpendicular to the (001) direction.[13,14] The films were characterized *in situ* by reflection high-energy electron diffraction, and *ex situ* by x-ray diffraction, atomic force micros-

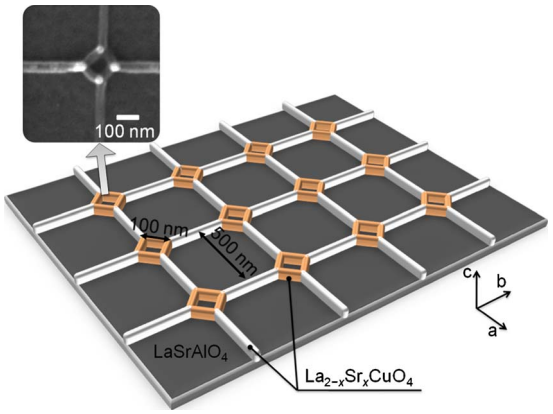

FIG. 1. (Color online) Main panel: schematic description of a sample consisting of 100×100 nm^2 loops (orange color) interconnected by 500 nm long wires (bright bars). Inset: SEM image of a single loop patterned by electron-beam lithography in a $La_{1.84}Sr_{0.16}CuO_4$ film. The whole sample contains 60×60 small loops.

copy and mutual inductance measurements. Subsequently, the films were patterned into a 30×30 μm^2 network consisting of 100×100 nm^2 square loops with ~25 nm wire width, separated by 500×500 nm^2 loops, as shown schematically in Fig. 1. We note that the size of the loops and the wire width in the present experiment are nearly an order of magnitude smaller than previously studied in high-T_c networks and rings.[7,15–19] In this specially designed network the small loops do not share sides, thus eliminating complications that may arise in simple networks (e.g., a square network), such as vortex interaction and frustration or interstitial vortices trapped in the wires.[5–7,15–18] Simulations[20] show that the decoupling of the small loops improves as the ratio between the sides of the large and the small loops increases. In the present network we achieved a ratio of 5:1 as compared to about 3:1 in our previous published work.[8] In such a network, the behavior of the small loops approximates that of an ensemble of isolated loops, thus reflecting the behavior of a single loop. Nevertheless, this decoupled network has an advantage over a single loop as it allows application of larger currents, thus improving the signal-to-noise ratio. In addition, measurements on large number of loops in the network average effects of inhomogeneities and size distribution.

The network pattern of Fig. 1 was created using a CRESTEC Cable-9000C high resolution e-beam lithography system in a layer of poly(methyl methacrylate) (PMMA) resist spun-off on top of a superconducting $La_{1.84}Sr_{0.16}CuO_4$ film. This PMMA pattern served as a mask for transferring the pattern to the superconducting film by Ar-ion milling. The scanning electron microscope (SEM) image in the inset shows a detail (a single loop) of the resulting superconducting network. The network magnetoresistance was measured using a Quantum Design physical properties measurement system. The magnetic field was applied normal to the film surface (the *a*-*b* crystallographic plane) and the bias current was 1 μA.

Figure 2 shows measurements of the network resistance $R(T)$ at zero field as a function of temperature before (closed circles) and after (open circles) patterning. Evidently, pat-

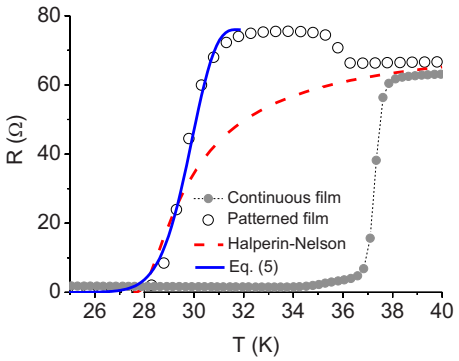

FIG. 2. (Color online) Measured temperature dependence of the resistance in a continuous film (solid circles, the dotted line is a guide to the eyes) and the patterned film (open circles) at zero applied field. The solid blue line is calculated using Eq. (5) with $T_c=32$ K and $R_n=76$ Ω yielding fit values $\lambda_0=750$ nm, $\xi_0=2.5$ nm, $d=23.4$ nm, and $w=21$ nm. The red dashed line is based on the Halperin-Nelson formula for a 2D superconductor (Ref. 21) using the Berezinski-Kosterlitz-Thouless transition temperature, $T_{BKT}=27.6$ K, the fluctuation-corrected BCS critical temperature, $T_{BCS}=32$ K, and $R_n=76$ Ω.

terning of the film into narrow wires causes broadening of the resistive transition. In the following we show that this broadening can be interpreted as the result of a decrease in energy required to create a vortex/antivortex pair as the wire width decreases. Figure 2 also shows an anomalous peak in $R(T)$ of the patterned film near T_c. A similar peak was observed previously in superconducting nanostructures and its origin is still debated.[22–24]

Figure 3 shows the network magnetoresistance measured at different temperatures between 27 and 32 K. The measured magnetoresistance exhibits large oscillations superimposed on a monotonic background. The temperature up to which the oscillations persist, which in what follows we define as the transition temperature, T_c, is ~32 K. The oscillation amplitude decreases as the field increases. At temperatures above ~32 K, $R(H)$ exhibits an anomalous shape, the magnetoresistance is decreasing with the field (negative magnetoresistance).[25] The period of the oscillations, $H_0\approx2300$ Oe, corresponds to the magnetic flux quantum, $H_0=\Phi_0/\pi r^2$, where $r\approx52.8$ nm is the effective radius of the

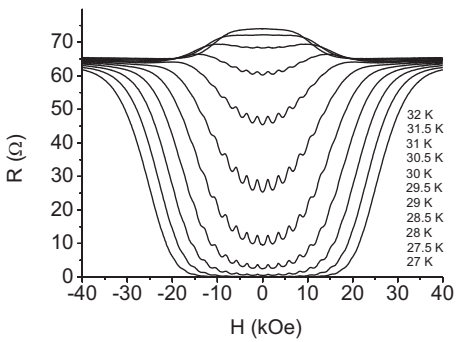

FIG. 3. Resistance of the patterned film as a function of magnetic field perpendicular to the sample plane (i.e., parallel to the *c*-crystallographic axis) at different temperatures. The lowest and the uppermost curves correspond to 27 K and 32 K, respectively.

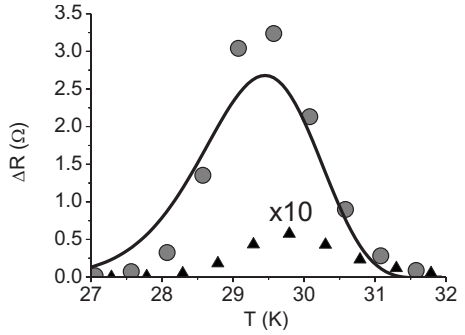

FIG. 4. Temperature dependence of the measured oscillation amplitude (circles). The solid line is calculated using Eq. (7) with the parameters extracted from Fig. 2. The triangles show an upper limit for the resistance oscillations amplitude calculated for the Little-Parks effect; note that this scale is expanded tenfold.

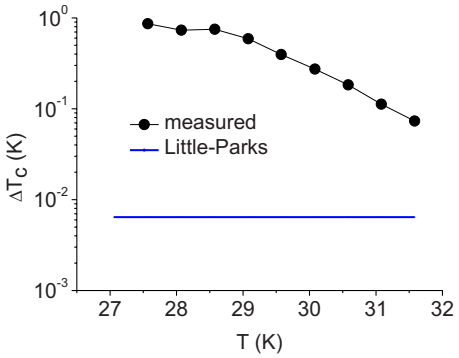

FIG. 5. (Color online) Solid circles: the amplitude of oscillations in T_c, $\Delta T_c = \Delta R(H)(dT/dR)$, derived from the experimentally measured oscillation amplitude, ΔR, and the temperature derivative dR/dT. The solid black line connecting the experimental points is a guide to the eyes. The solid blue line presents the change in T_c, ΔT_c^{LP}, that one would expect from the Little-Parks effect. Note that the two scales differ by 2 orders of magnitude.

small loop. Oscillations of the period ~80 Oe corresponding to the large loops are also observed but on the scale of Fig. 3 their amplitude is too small to be noticed. In Fig. 4, the circles show the measured temperature dependence of the oscillations amplitude. Evidently, the magnetoresistance oscillations are observed only within a limited temperature range around the transition, exhibiting the maximum amplitude around 29.5 K.

III. THEORETICAL MODEL AND DISCUSSION

The magnetoresistance oscillations shown in Fig. 3 at the first sight resemble the Little-Parks effect[2,3] originating from the periodic dependence of the critical temperature, T_c, on the applied magnetic field. However, this resemblance is deceptive. For an estimate, let us take as the typical[26] value of the coherence length, $\xi_0 = 2$ nm, the critical temperature in zero field at the onset of the resistance drop, $T_c = 32$ K, and the loop effective radius $r = [\Phi_0/(\pi H_0)]^{1/2} = 52.8$ nm; using these parameter values for the amplitude of oscillations in T_c one obtains[11,27] $\Delta T_c^{LP} = 0.14 T_c (\xi_0/r)^2 \approx 6.4$ mK. From this ΔT_c^{LP} we can calculate an upper limit to the resistance oscillations amplitude, $\Delta R = \Delta T_c^{LP}(dR/dT)$, shown by the triangles in Fig. 4. Evidently, ΔR expected from the Little-Parks effect exhibits the maximum value which is a factor of ~50 smaller than the maximum value measured in our experiment. Moreover, attributing the data shown in Fig. 3 to the Little-Parks effect leads to the illogical conclusion that ΔT_c^{LP} would be temperature dependent. This is shown in Fig. 5, where the solid points were calculated from the experimentally measured oscillation amplitude, ΔR, and the temperature derivative dR/dT, using $\Delta T_c = \Delta R/(dR/dT)$. Note that the extracted ΔT_c exhibits unexpected temperature dependence with values that are two orders of magnitude larger than the constant value of about 6.4 mK (the solid line in Fig. 5).[28]

Given that the Little-Parks effect cannot explain the observed giant magnetoresistance oscillations, one needs to look for alternative explanations. We conjecture that the origin of this phenomenon may be in drastically modified vortex dynamics in nanopatterned films. While in continuous films the activation energy for vortex creep usually decreases monotonically with the applied magnetic field,[29–31] in nanopatterned films this activation energy becomes oscillatory, since moving vortices interact with the current induced in nanoloops, and this current is a periodic function of the field strength. Periodicity of the induced current results directly from the fluxoid quantization[1–3,27] which is also the cause of the Little-Parks effect. The fluxoid, consisting of the flux induced by the supercurrent in the loop and by the external magnetic field, is characterized by the quantum vorticity number, N, which defines the energy state of the superconducting loop. In the lowest energy state, N is equal[11,27] to H/H_0 rounded to the nearest integer. Thermally induced vortices or antivortices cause fluxoid transitions from the equilibrium quantum state, N, to a higher energy state. Kirtley *et al.*[9] and Kogan *et al.*,[10] in their analysis of magnetic scanning microscope measurements of mesoscopic superconducting rings, calculated the energies $\Delta E_{in}^{\pm}$ and $\Delta E_{out}^{\pm}$ that are required to create a vortex (+) or an antivortex (−) in a superconducting wire forming a loop and to carry it into or outside of the loop hole, respectively,

$$\Delta E_{in}^{\pm} = E_v(T) + E_0(T)(N - H/H_0 + 1/2) \mp \mu H,$$

$$\Delta E_{out}^{\pm} = E_v(T) + E_0(T)(N - H/H_0 - 1/2) \mp \mu H. \quad (1)$$

The first term in Eq. (1), E_v, is field independent and represents the energy needed for creation of the vortex/antivortex in a ring with annulus width w. For our rings with $r/w > 1/2$ we can use $E_v = \Phi_0^2 \ln[2w/\pi\xi(T)]/8\pi^2\Lambda(T)$. Here, $\xi(T) = 0.74\xi_0(1 - T/T_c)^{-1/2}$ is the Ginzburg-Landau coherence length[11] and $\Lambda(T) = 2\lambda(T)^2/d$ the Pearl penetration depth[11,32] in a film of thickness d and with the London penetration depth[11] $\lambda(T) = \lambda_0[1 - (T/T_c)^2]^{-1/2}$.

The second term in Eq. (1) is periodic with the field, expressing the interaction of a vortex or an antivortex with the current associated with the fluxoid in terms of the energy E_0. For our rings we use $E_0 = \Phi_0^2 \ln[(r+w/2)/(r-w/2)]/8\pi^2\Lambda(T)$. The quantized values of N lead to periodi-

cally oscillating values of $(N-H/H_0)$. The third term in Eq. (1) is the energy of the magnetic dipole moment, $\mu(T)=\Phi_0 w^2/32\pi\Lambda(T)$, associated with a vortex or an antivortex.[33]

As fluxoid transitions of higher order, $N\rightarrow N+m$ with $|m|\geq 2$, are statistically less significant, we consider fluxoid transitions accomplished by only *one* vortex or antivortex entry or exit. Thermodynamic averaging over the above four types of excitation energies, ΔE_i^j, yields an effective potential barrier, $\langle\Delta E\rangle$,

$$\langle\Delta E\rangle = \sum_{\substack{i\in in,out \\ j\in +,-}} \Delta E_i^j e^{-\Delta E_i^j/k_BT} \Bigg/ \sum_{\substack{i\in in,out \\ j\in +,-}} e^{-\Delta E_i^j/k_BT}. \quad (2)$$

Using Eq. (1) one obtains

$$\begin{aligned}\langle\Delta E(T,H)\rangle &= E_v + E_0/2 - E_0(N-H/H_0)\tanh\left[\frac{E_0(N-H/H_0)}{k_BT}\right] \\ &\quad - \mu H \tanh\left(\frac{\mu H}{k_BT}\right) \\ &\approx E_v - E_0(N-H/H_0)\tanh \\ &\quad \times\left[\frac{E_0(N-H/H_0)}{k_BT}\right] - \mu H \tanh\left(\frac{\mu H}{k_BT}\right). \quad (3)\end{aligned}$$

In the approximations made in Eq. (3) we assumed that $E_v \gg E_0$, which is especially valid for narrow rings, $r\gg w$. The first term in Eq. (3), $E_v(T)$, describes the zero-field excitation energy as a function of temperature, since the other two terms vanish at zero magnetic field. The second term describes the periodic part and the third term is responsible for the monotonic field-dependent "background" (see Fig. 3). Note that in this model E_v, E_0, and μ depend only on temperature.

In the next step, we derive the magnetoresistance following Tinkham's approach in his analysis[29] of the resistive transition in high-T_c superconductors. Replacing the activation energy in his equations with $\langle\Delta E\rangle$ as given in Eq. (3) yields

$$\frac{R}{R_n} = \left[I_0\left(\frac{\langle\Delta E\rangle}{2k_BT}\right)\right]^{-2}, \quad (4)$$

where I_0 is the zero-order modified Bessel function of the first kind. In the following, we show that Eq. (4) in conjunction with Eq. (3) can explain a rich variety of phenomena, including the observed transition broadening, the oscillations of magnetoresistance, the temperature dependence of the oscillation amplitude, and the shape of the monotonic background on which the magnetoresistance oscillations are superimposed.

Equations (1)–(4) are applicable to a single loop of radius r and can also apply to a wire for which $r\rightarrow\infty$. In applying these equations to a network of decoupled loops interconnected by relatively long wires (see Fig. 1), we note that the total resistance of such a network is $R=R^{loop}+R^{wire}$, where R^{loop} and R^{wire} are the resistances of a small loop and of a single interconnecting wire, respectively. Expressions for R^{loop} and R^{wire} can be obtained on the basis of Eq. (4),

$$R = R_n^{loop}\left[I_0\left(\frac{\langle\Delta E^{loop}\rangle}{2k_BT}\right)\right]^{-2} + R_n^{wire}\left[I_0\left(\frac{\langle\Delta E^{wire}\rangle}{2k_BT}\right)\right]^{-2}, \quad (5)$$

where $\langle\Delta E^{loop}\rangle$ and $\langle\Delta E^{wire}\rangle$ are given in Eq. (3) by including and omitting the E_0 term, respectively. (The term E_0 is responsible for the oscillations that are absent in the wires.) For the network described in Fig. 1, R^{loop} and R^{wire} are 22% and 78%, respectively, of the measured $R_n=76\ \Omega$ at $T_c=32$ K, reflecting the relative lengths of the short and the long wires in the network.

A. Transition broadening at zero field

The solid blue line in Fig. 2 shows a fit to the data points of the resistance in a patterned film in the transition region, using Eq. (5) in the zero-field limit. Note that in this limit $\langle\Delta E^{loop}\rangle$ and $\langle\Delta E^{wire}\rangle$ reduce to $E_v(T)$. This fit yields $d=23.4$ nm, $w=21$ nm, $T_c=32$ K, $R_n=76\ \Omega$, $\lambda_0=750$ nm, and $\xi_0=2.5$ nm. The calculated resistance is in a reasonably good agreement with the experimental data, indicating that the transition broadening is primarily due to enhanced vortex motion across narrow wires due to reduced E_v. Equation (5) does not account for the anomalous resistive peak observed at elevated temperatures. A similar peak was observed in other superconducting nanostructures[22–24] but its origin is still controversial.

The dashed line in Fig. 2 shows an attempt to fit the resistance data of the patterned film to the Halperin-Nelson formula for 2D superconductors, based on vortex-antivortex unbinding.[21] In the calculation of this curve we assumed a BKT transition temperature, $T_{\mathrm{BKT}}=27.5$ K, and the "fluctuation-corrected BCS critical temperature," $T_{\mathrm{BCS}}=32$ K. Apparently, this model does not account for the temperature dependence of the magnetoresistance measured in our nanoloops except for a limited temperature range in the immediate vicinity of ~27.5 K. At higher temperatures the Halperin-Nelson formula describes "fluctuation-corrected BCS behavior," which does not explain our results.

B. Oscillations amplitude—temperature dependence

As the origin of the oscillations is in the small loops, in the following we derive an expression for the oscillations amplitude based on Eq. (3). We apply this equation for low fields such that the term $-\mu H\tanh(\mu H/k_BT)$ in the excitation energy [Eq. (3)] is small compared to E_v. Using the approximation $\tanh[E_0(N-H/H_0)/k_BT]\approx E_0(N-H/H_0)/k_BT$ in the periodic term, one obtains

$$\frac{R}{R_n} \approx [I_0\{E_v/2k_BT - [E_0(N-H/H_0)/k_BT]^2/2\}]^{-2}, \quad (6)$$

which is an oscillating function of the magnetic field.

One can approximate the amplitude of the oscillations, $\Delta R(T)$, as the difference between the zero-field curve, $R(T,H=0)$, and the shifted resistance curve $R(T,H=H_0/2)$. If the difference is relatively small, ΔR can be approximated as

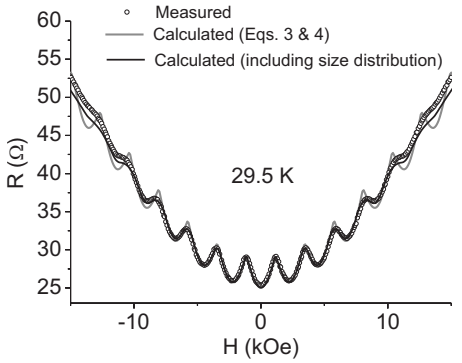

FIG. 6. Magnetoresistance oscillations at 29.5 K: measured (open circles) and calculated using Eq. (5) (the solid gray line). The solid black line is calculated with the same equations but assuming a size distribution of the loops, resulting in the spread of ±8% in H_0 around the mean value of ~2300 Oe.

$$\Delta R \approx \left.\frac{dR}{d\langle E\rangle}\right|_{H=0} \Delta E = R_n \frac{I_1(E_v/2k_BT)}{I_0[E_v/2k_BT]^3}\left[\frac{E_0}{2k_BT}\right]^2, \quad (7)$$

where ΔE is the amplitude of periodic change in the excitation energy with the field and I_1 is the first-order modified Bessel function of the first kind. This equation, which was derived for a single loop, is also valid for the network if we replace R_n with R_n^{loop}, because the origin of oscillations is in the small loops.

We note that E_v and E_0 are functions of two length scales, λ_0 and ξ_0. The calculated amplitude, using Eq. (7) with λ_0 =750 nm, ξ_0=2.5 nm, r=52.8 nm, d=23.4 nm, and w =21 nm, is shown as the solid line in Fig. 4. A fairly good agreement between the experimental data and the theoretical curve is obtained. We note that the values of the parameters λ_0 and ξ_0 may be influenced by the lithography process, which may cause damage in regions near the surface and sides and make the effective thickness and width significantly smaller than the nominal values.

It should be mentioned that an earlier work has found large-amplitude magnetoresistance oscillations in a different nanostructure made of two low-T_c superconducting nanowires.[34,35] These oscillations were attributed to the field-driven modulation of barrier heights for phase slips. As that interpretation relates to one-dimensional superconducting wires ($w < \xi$), it may not be directly applicable to our high-T_c loops in which the wire width is an order of magnitude larger than the coherence length.

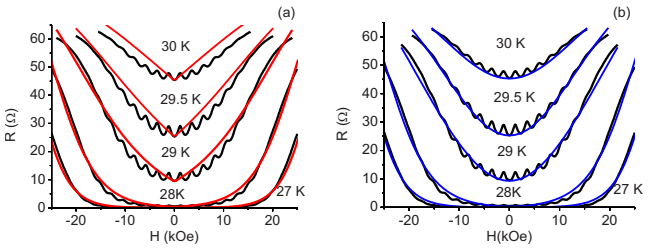

FIG. 7. (Color online) Theoretical fits of the nonoscillating background (the line connecting the *minima* of the oscillatory magnetoresistance) to the experimental data (black lines) taking into account (a) only vortices (left panel, red lines) and (b) both vortices and antivortices (right panel, blue lines).

C. Magnetoresistance oscillations—field dependence

Figure 6 shows a comparison of the field dependence of magnetoresistance measured at 29.5 K (open circles) with the one calculated using Eq. (5) (the solid gray line) and taking E_v=94 and E_0=72 in the units of k_B and μ=28 in the units of k_B/T. A good agreement between the calculated curve and the experimental data is seen only at low fields. As the field increases, the experimentally measured amplitude decreases while the calculated amplitude remains almost constant. The agreement between the theory and the experiment can be extended to high fields if we take into account the distribution of the size of loops in the patterned film. As loops of different size give different period of oscillations, averaging over a size distribution of the small loops causes a decrease in the oscillations amplitude. We can account for this size spread assuming an equal-size distribution of ±8% around the median value of 52.8 nm and then average over the contributions to $R(H)$ from loops of different sizes. This procedure yields a good fit (the solid black curve in Fig. 6) over a large field range.

It should be noted that a decay of the magnetoresistance oscillations at high fields was observed not only in networks[5–7] but also in low-T_c cylinders[2–4] and, more recently, in a high-T_c superconducting single ring.[19] The latter observation may be ascribed to variation in the order parameter along the radial direction across the relatively wide ring (270–300 nm), creating a discrete number of concentric independent domains where supercurrent density is different from zero.[19] In low-T_c cylinders[2–4] the oscillations originate from the Little-Parks effect, i.e., from the changes in T_c with field. The resulting magnetoresistance changes are proportional to dR/dT which decreases as the field increases.

TABLE I. The values of E_v and μ at different temperatures.

T (K)	E_v (K)	μ (K/T)	$E_v/2k_BT$	$\mu/2k_BT$ (1/T)	
30	63	21	1.1	0.4	} < 1
29.5	93.5	30	1.6	0.5	
29	134	41	2.3	0.7	
28	243	77	4.3	1.4	} > 1
27	349	104	6.5	1.9	

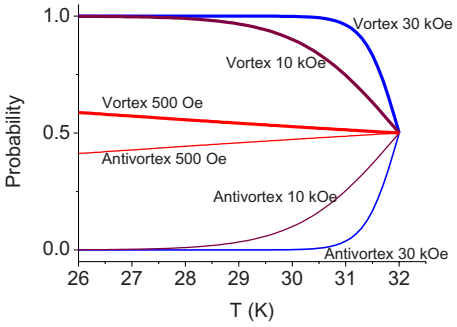

FIG. 8. (Color online) The calculated probabilities of thermally induced creation of a vortex (solid lines) and an antivortex (thin solid lines) as functions of the magnetic field.

D. Monotonic field background

We define the background as the line connecting the minima points of the oscillatory magnetoresistance. Thus, in calculating the background, the periodic term included in $\langle \Delta E^{loop} \rangle$ of Eq. (5) is neglected as it takes zero value at fields mH_0 with integer m. Assuming that only vortices are present in the system the resistance would be

$$R_{backgr} = R_n^{loop}\{I_0[(E_0 - \mu|H|)/(2k_BT)]\}^{-2} + R_n^{wire}\{I_0[-\mu|H|/(2k_BT)]\}^{-2}. \quad (8)$$

In the presence of *both* vortices and antivortices, $\mu|H|$ in Eq. (8) has to be replaced by $\mu H \tanh(\mu H/k_BT)$. Two fits of expression (8) to the experimental data at different temperatures are shown in Figs. 7(a) and 7(b), the first assuming the presence of vortices alone and the second assuming the presence of both vortices and antivortices. It can be seen clearly that taking into account only vortices fails to explain the background at temperatures above ~28.5 K while taking into account both vortices and antivortices provides a much better description of the experimental results.

The fits shown in Fig. 7(b) yield the values of E_v and μ at different temperatures listed in Table I. These values decrease with temperature as predicted in Ref. 33 and are of same order of magnitude as the calculated values of $E_v = \Phi_0^2 \ln[2w/\pi\xi(T)]/8\pi^2\Lambda(T)$ and $\mu(T) = \Phi_0 w^2/32\pi\Lambda(T)$.

The need to account for antivortices in explaining the magnetoresistance background at high temperatures becomes apparent by considering the probabilities P_V and P_{AV} of thermally excited vortex and antivortex in a superconducting wire. These can be expressed as $P_V(T,H) \propto \exp[-(E_V - \mu|H|)/k_BT]$ and $P_{AV}(T,H) \propto \exp[-(E_V + \mu|H|)/k_BT]$, respectively. In Fig. 8 we show the calculated P_V and P_{AV} as a function of temperature for different fields. From these curves it is clear that at high magnetic fields the probability of antivortices is highly suppressed. However, at sufficiently high temperatures antivortices occur with a relatively high probability even at high fields.

IV. SUMMARY AND CONCLUSIONS

In uniform (unpatterned) films the activation energy for vortex creep usually decreases monotonically with the applied magnetic field.[29–31] In contrast, in films nanopatterned into a network of loops, this activation energy becomes oscillatory, because moving vortices interact with the periodically oscillating current induced in the loops. The activation energy also includes a term that varies monotonically with the applied field because of magnetic interaction of vortices and antivortices with the applied field. The combination of monotonic and oscillatory terms of the activation energy gives rise to magnetoresistance oscillations superimposed on a monotonically increasing background. On the basis of this model, we have derived analytical expressions for the magnetoresistance oscillations and for the background and showed good quantitative agreement with the experimental results obtained from an array of noninteracting nanosized loops in a $La_{1.84}Sr_{0.16}CuO_4$ film.

In analyzing the monotonic background of magnetoresistance we showed that it is necessary to account for the presence in the film of antivortices alongside with vortices, especially at elevated temperatures. This finding may have an implication on the debated BKT transition, which predicts dissociation of vortex-antivortex pairs above the transition temperature in thin superconducting films. Further study of the possibility of manifestation of Berezinskii-Kosterlitz-Thouless transition in our experiment requires an extension of our analysis to include the contribution of vortex-(anti)vortex interactions to the activation energy.

ACKNOWLEDGMENTS

We thank A. Bollinger, A. Frydman, A. Gozar, L. Klein, V. V. Kogan, J. Mannhart, Y. Oreg, O. Pelleg, Z. Radović, B. Rosenstein, B. Ya. Shapiro, E. Shimshoni, V. Vinokur, and E. Zeldov for helpful discussions. The work at Bar-Ilan University was supported by the Deutsche Forschungsgemeinschaft through the Deutsch Israelische Projektkooperation (Grant No. 563363). Y.Y. acknowledges support of the Israel Science Foundation. I.S. thanks the Israeli Ministry of Science and Technology. The work at BNL was supported by US DOE under Contract No. MA-509-MACA.

[1] F. London, Phys. Rev. **74**, 562 (1948).
[2] W. A. Little and R. D. Parks, Phys. Rev. Lett. **9**, 9 (1962).
[3] R. D. Parks and W. A. Little, Phys. Rev. **133**, A97 (1964).
[4] R. P. Groff and R. D. Parks, Phys. Rev. **176**, 567 (1968).
[5] An extensive literature on the Little-Parks effect in low-T_c materials can be found in Proceedings of the NATO Workshop on Conference in Superconducting Networks, Delft, The Netherlands, edited by J. E. Mooij and G. B. J. Schon, 1987 [Physica B **152**(1-2) (1988)].
[6] A. Behrooz, M. J. Burns, D. Levine, B. Whitehead, and P. M. Chaikin, Phys. Rev. B **35**, 8396 (1987).
[7] P. L. Gammel, P. A. Polakos, C. E. Rice, L. R. Harriott, and D. J.

Bishop, Phys. Rev. B **41**, 2593 (1990).
[8] I. Sochnikov, A. Shaulov, Y. Yeshurun, G. Logvenov, and I. Bozovic, Nat. Nanotechnol. **5**, 516 (2010).
[9] J. R. Kirtley, C. C. Tsuei, V. G. Kogan, J. R. Clem, H. Raffy, and Z. Z. Li, Phys. Rev. B **68**, 214505 (2003).
[10] V. G. Kogan, J. R. Clem, and R. G. Mints, Phys. Rev. B **69**, 064516 (2004).
[11] M. Tinkham, *Introduction to Superconductivity* (McGraw-Hill, New York, 1996).
[12] D. R. Strachan, C. J. Lobb, and R. S. Newrock, Phys. Rev. B **67**, 174517 (2003).
[13] I. Bozovic, IEEE Trans. Appl. Supercond. **11**, 2686 (2001).
[14] I. Bozovic, G. Logvenov, I. Belca, B. Narimbetov, and I. Sveklo, Phys. Rev. Lett. **89**, 107001 (2002).
[15] A. Castellanos, R. Wordenweber, G. Ockenfuss, A. d. Hart, and K. Keck, Appl. Phys. Lett. **71**, 962 (1997).
[16] A. Crisan, A. Pross, D. Cole, S. J. Bending, R. Wordenweber, P. Lahl, and E. H. Brandt, Phys. Rev. B **71**, 144504 (2005).
[17] S. Ooi, T. Mochiku, S. Yu, E. S. Sadki, and K. Hirata, Physica C **426-431**, 113 (2005).
[18] S. Goldberg, Y. Segev, Y. Myasoedov, I. Gutman, N. Avraham, M. Rappaport, E. Zeldov, T. Tamegai, C. W. Hicks, and K. A. Moler, Phys. Rev. B **79**, 064523 (2009).
[19] F. Carillo, G. Papari, D. Stornaiuolo, D. Born, D. Montemurro, P. Pingue, F. Beltram, and F. Tafuri, Phys. Rev. B **81**, 054505 (2010).
[20] I. Sochnikov (unpublished).
[21] B. I. Halperin and D. R. Nelson, J. Low Temp. Phys. **36**, 599 (1979).
[22] I. L. Landau and L. Rinderer, Phys. Rev. B **56**, 6348 (1997).
[23] P. Santhanam, C. C. Chi, S. J. Wind, M. J. Brady, and J. J. Bucchignano, Phys. Rev. Lett. **66**, 2254 (1991).
[24] C. Strunk, V. Bruyndoncx, C. Van Haesendonck, V. V. Moshchalkov, Y. Bruynseraede, C. J. Chien, B. Burk, and V. Chandrasekhar, Phys. Rev. B **57**, 10854 (1998).
[25] The sensitivity of the resistance to the magnetic field above 32 K may suggest that some parts of the array are superconducting already below 35 K, see Refs. 22–24 and 36.
[26] H. H. Wen, H. P. Yang, S. L. Li, X. H. Zeng, A. A. Soukiassian, W. D. Si, and X. X. Xi, Europhys. Lett. **64**, 790 (2003).
[27] M. Tinkham, Rev. Mod. Phys. **36**, 268 (1964).
[28] Discrepancies between the Little-Parks model and the experimental results, namely, the magnitude of magnetoresistance oscillations and their anomalous temperature dependence, were already observed in low-T_c superconductors (e.g., in Refs. 2 and 3). In our case, however, the discrepancies amount to 2 orders of magnitude, much larger than observed in low-T_c materials, indicating a different underlying physics.
[29] M. Tinkham, Phys. Rev. Lett. **61**, 1658 (1988).
[30] G. Blatter, M. V. Feigel'man, V. B. Geshkenbein, A. I. Larkin, and V. M. Vinokur, Rev. Mod. Phys. **66**, 1125 (1994).
[31] Y. Yeshurun, A. P. Malozemoff, and A. Shaulov, Rev. Mod. Phys. **68**, 911 (1996).
[32] J. Pearl, Appl. Phys. Lett. **5**, 65 (1964).
[33] V. G. Kogan, Phys. Rev. B **49**, 15874 (1994).
[34] D. S. Hopkins, D. Pekker, P. M. Goldbart, and A. Bezryadin, Science **308**, 1762 (2005).
[35] D. Pekker, A. Bezryadin, D. S. Hopkins, and P. M. Goldbart, Phys. Rev. B **72**, 104517 (2005).
[36] D. Y. Vodolazov, D. S. Golubović, F. M. Peeters, and V. V. Moshchalkov, Phys. Rev. B **76**, 134505 (2007).